◆ Human Brain Mapping 30:3031–3042 (2009) ◆

Cardiorespiratory Effects on Default-Mode Network Activity as Measured With fMRI

Mariët van Buuren,[1]* Thomas E. Gladwin,[1,2] Bram B. Zandbelt,[1] Martijn van den Heuvel,[1] Nick F. Ramsey,[3] René S. Kahn,[1] and Matthijs Vink[1]

[1]*Rudolf Magnus Institute of Neuroscience, Department of Psychiatry, University Medical Center Utrecht, Utrecht, The Netherlands*
[2]*Stuivenberg Hospital, Department of Psychiatry, Antwerp, Belgium*
[3]*Rudolf Magnus Institute of Neuroscience, Department of Neurosurgery, University Medical Center Utrecht, Utrecht, The Netherlands*

Abstract: The default-mode network (DMN) consists of areas showing more activation during rest than during a task. Several authors propose some form of cognitive processing to underlie BOLD signal changes in the DMN as activity within the network is modulated by the level of effort required by the task and is positively correlated with self-referential processing. Alternatively, BOLD signal changes within the DMN may be caused by cardiorespiratory processes (CR) affecting BOLD signal measurements independent of neuronal activity. The goal of this study is to investigate whether BOLD signal changes within the DMN can be explained by CR effects. To this aim, brain activity, heartbeat, and respiration are measured during resting-state and while subjects perform a cognitive task with a high- and low-demand condition. To correct for CR effects we used RETROICOR (Glover et al., [2000]: Magn Reson Med 44:162–167) in combination with additive linear modeling of changes due to respiration volume, heart rate and heart rate variability. CR effects were present within the frequency-range of the DMN and were located in areas of the DMN, but equally so in other areas. After removal of CR effects, deactivation and resting-state connectivity between the areas of the DMN remained significant. In addition, DMN deactivation was still modulated by task demand. The same CR correction method did remove activation in task-related areas. We take these results to indicate that the BOLD signal within the DMN cannot be explained by CR effects alone and is possibly related to some form of cognitive neuronal processing. *Hum Brain Mapp 30:3031–3042, 2009.*

Key words: fMRI; default-mode network; respiration; heart rate; functional connectivity; resting-state

INTRODUCTION

Functional imaging studies typically investigate brain function by identifying areas showing increased activation during a task as compared to rest or baseline. However, some areas in the brain are more active during rest [Binder et al., 1999; Mazoyer et al., 2001; Shulman et al., 1997]. Together, these areas are called the default-mode network (DMN) and include the posterior cingulate (PCC), the medial prefrontal cortices and the lateral posterior cortices (Brodmann area 39) [Fox et al., 2005; Greicius et al., 2003; Raichle et al., 2001]. Functional connectivity studies have

*Correspondence to: Mariët van Buuren, Rudolf Magnus Institute of Neuroscience, University Medical Center Utrecht, Room A.01.126, PO Box 85500, NL-3508 GA Utrecht, The Netherlands.
E-mail: m.vanbuuren-2@umcutrecht.nl

Received for publication 8 July 2008; Revised 4 December 2008; Accepted 8 December 2008

DOI: 10.1002/hbm.20729

Published online 29 January 2009 in Wiley InterScience (www.interscience.wiley.com).

found positive correlations between the areas of this network in low-frequency bands from around 0.01 to 0.1 Hz during resting-state fMRI, indicating that activity within this network is correlated [Damoiseaux et al., 2006; Fox et al., 2005; Greicius et al., 2003; Lowe et al., 1998].

Several authors propose some form of cognitive processing to underlie BOLD signal changes in the DMN, as these signal changes are modulated by the level of effort required to perform a task. That is, deactivation within the DMN increases relative to rest (i.e. activation decreases) as task-demand increases, suggesting that BOLD signal changes within the DMN are related to cognitive processes [McKiernan et al., 2003; McKiernan et al., 2006; Singh and Fawcett, 2008]. Later studies have extended this interpretation by showing positive correlations between BOLD signal changes in the DMN and self-referential mental processing [Gusnard et al., 2001; Gusnard and Raichle, 2001; Johnson et al., 2002], and mind-wandering [Mason et al., 2007].

However, another possible explanation is that BOLD signal changes within the DMN are caused, or at least obscured, by confounding cardiorespiratory processes (CR) affecting BOLD signal measurements independently from neuronal activity [Birn et al., 2006; Glover et al., 2000; Katura et al., 2006; Shmueli et al., 2007; Wise et al., 2004]. For example, the cardiac and respiratory cycle cause signal changes in brain areas near major vessels and the ventricles, and motion artifacts near the edges of the brain [Bhattacharyya and Lowe, 2004; Dagli et al., 1999; Glover et al., 2000; Hu et al., 1995]. In addition, fluctuations in heart rate (HR), heart rate variability (HRV) and respiration volume are related to BOLD signal changes in grey matter areas not located near large vessels [Birn et al., 2006; Critchley et al., 2003; Shmueli et al., 2007; Wise et al., 2004]. These CR effects may be particularly problematic for the interpretation of the BOLD signal within the DMN. That is, recent studies showed that respiration and HR related fluctuations in the BOLD signal were both present in the frequency range of the DMN ($\approx$0.03 Hz and $<$0.1 Hz, respectively) as well as located within areas of the DMN [Birn et al., 2006; Shmueli et al., 2007]. In addition to spontaneous CR processes, changes in CR processes can be related to task demands [Jorna et al., 1992], making the interpretation of task-induced BOLD signal changes difficult.

The goal of this study is to investigate whether resting-state and task-induced BOLD signal changes within the DMN can be explained by CR effects. To this aim, brain activity, heartbeat, and respiration are measured during resting-state and while subjects perform a cognitive task with two levels (high-/low-demand). To identify and correct for CR effects we used RETROICOR [Glover et al., 2000] in combination with regressors to model changes due to respiration volume, HR and HRV. Data from earlier studies suggest that filtering out CR effects will remove a significant portion of the BOLD signal within the DMN. Consequently, we expect to find (a) reduced deactivation within the DMN during the task and (b) a reduction in resting-state connectivity after correcting for CR effects. However, if the residual BOLD signal within the DMN remains correlated during resting-state and still shows a task-demand related increase in deactivation, this may point towards some form of cognitive neuronal activity. In all analyses, a network consisting of areas showing activation during the cognitive task (i.e. task-positive network) is included to compare the effects of CR correction on the BOLD signal within this network to those within the DMN.

METHODS

Participants

Fourteen right-handed (mean $\pm$ SD Edinburgh Handedness Inventory [Oldfield, 1971] quotient, 0.84 $\pm$ 0.15) male subjects (mean $\pm$ SD years, 22.8 $\pm$ 2.3) were included in this study. None of the participants had a history of psychiatric or neurological disorders, medication use, substance abuse or medical disorders or had any contraindications for MRI. Participants were recruited from the University of Utrecht and received monetary compensation for participation. All gave written informed consent. The ethics committee of the University Medical Center of Utrecht approved this study.

Tasks

Target detection task

In the target detection task [visual oddball task, e.g. Kiehl et al., 2001; Yoshiura et al., 1999], subjects were instructed to respond, by pressing a button, to target stimuli which appeared within a series of nontargets (see Fig. 1). The task consisted of 10 blocks (of 30 s each) of 30 trials

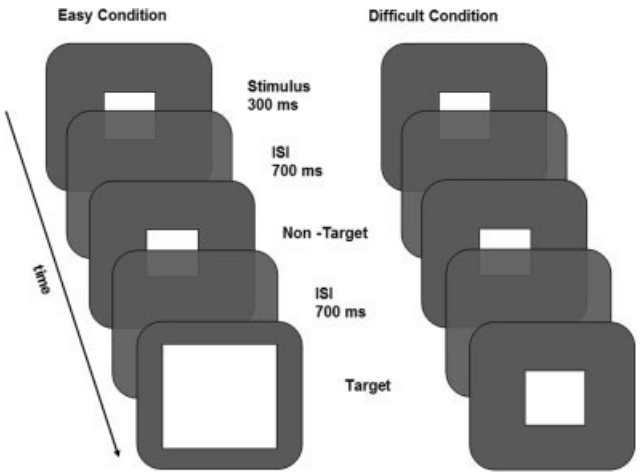

Figure 1.
Target detection task. In the easy condition, targets were 220% the size of the nontarget, whereas in the difficult condition target-size was 110% or 115% of that of the nontarget. ISI = inter stimulus interval.

(one instruction trial, nine targets, and 20 nontargets) alternated with rest periods of 30 s. In five out the 10 task blocks, targets were more than twice (220%) the size of the nontargets (i.e. easy condition), whereas in the other five blocks target-size was 110 or 115% of that of the nontargets (i.e. difficult condition). The exact size of the difficult target was individually determined by performance on a threshold task (see below). Before each block, the word 'easy' or 'difficult' was presented to indicate the onset of each condition (i.e. instruction trial). The order of the blocks was counterbalanced over the experiment. Within each block, the order of the stimuli was randomized, with the restrictions that a target stimulus had to be followed by a nontarget stimulus and that the first three stimuli were nontarget stimuli.

Before the target detection task, subjects performed a threshold task which consisted of 11 blocks (of 30 s each). In total, five different sizes for targets were used (110, 115, 120, 130, and 220% of the size of the nontarget). For the difficult task condition, the smallest target size was selected on which a subject scored 55% or more correct.

Resting-state

During a resting-state period of 6 min, subjects were instructed to look at a crosshair presented in the middle of the screen. Fox et al. [2005] showed that results obtained in this type of resting-state condition do not differ from results of conditions where a subject has the eyes closed or the eyes open without fixation. In addition, by presenting a fixation cross, subjects have less difficulty to remain awake and eye-movements are limited, hence intersubject variability is restricted.

Cardiorespiratory Processes

Measurements

For measuring CR processes, four electrocardiogram electrodes were affixed to the subjects' chest and a respiration band was placed at the level of the abdomen. The measured CR data consisted of two signals, both sampled at 500 Hz: a heart beat signal with a trigger marking times at which an R-peak was detected, and a respiratory signal measuring the expansion of the respiration band. For the heart beat signal, a beat was inserted halfway between the triggers if an interbeat interval (IBI) was longer than 1.5 and the second trigger was deleted if an IBI was shorter than 500 ms to correct for artifacts.

Five measures were derived from these measured signals. (1) Cardiac phase. A phase ranging from 0 to 2 pi radians was assigned to every sample. The phase was linearly interpolated from the previous to the next heart beat trigger. (2) Respiration phase. Phases from -pi to +pi were assigned to every sample as follows [see also Glover et al., 2000]. First, the respiration signal was normalized to the range of 0 to 1, by adding the minimum value and then dividing by the new maximum value. The sorted values of the normalized respiration signal were divided into 100 bins with equally spaced bin centres. Next, the derivative of the normalized respiration signal was calculated by fitting a quadratic polynomial around the middle of 500 ms segments, and using the polynomial's derivative at every sample. Subsequently, for every sample, the number of samples with a lower or equal respiratory signal value was counted, based on the bin centres and number of values in the bins. This number was divided by the total number of samples in the respiration signal, and the proportion was multiplied by pi. Finally, the sign of the derivative was assigned to this value. For example, at the peak of inhalation, the phase rises to pi and then flips over to -pi. (3) HR. For every sample of the heart beat trigger signal, the associated IBI was calculated by determining the interval between the two surrounding heart beat triggers. This signal was subsequently used to create a smoothed HR signal. The mean IBI over 6 s intervals was calculated, and the HR at the sample at the center of that interval was defined as 1 divided by this mean IBI. The centers of each interval were shifted in 500 ms steps to avoid unnecessary computation time. The HR signal between the centers was filled in using linear interpolation. (4) HRV. HRV was calculated using the same sliding window as was used for HR. The variance of the IBIs during each 6 s interval was assigned to the central samples of the intervals, and linear interpolation was used to fill in the signal between them. (5) respiration volume per unit time (RVT). The RVT was calculated as in Birn et al. [2006]. For each sample, the amplitude and frequency of the current breath was calculated based on the exhalation and inhalation peaks. The amplitude was defined as the difference in value between the peaks, and the frequency was 1 divided by their distance in time. The RVT is the product of the amplitude and frequency.

The time courses of these five CR measures were down-sampled from 500 Hz to the sampling rate of the functional MRI scans (i.e. volumes) to obtain a CR time course at every scan. Down-sampling was conducted as follows. For the cardiac and respiration phase the sample at which each scan started was used and for HR, HRV, and RVT the mean from the start of the scan up to the start of the next scan was taken for each scan.

CR correction

The CR measures were divided into cyclic (cardiac phase and respiration phase) and noncyclic (HR, HRV, RVT) variables. All noncyclic variables and the functional MRI time courses were detrended using a basis set of cosines. The slowest cosine had a period of twice the signal length, and cosines with multiples of the initial frequency were added up to a period of 142 s. The cosines were fitted to the signal using multiple regression, and the explained signal was subtracted. Subsequently, the BOLD signal was corrected using the RETROICOR method [Glover et al., 2000]. This method

models the relationship between the phase of the cyclic variables and the BOLD signal of each voxel, and subtracts the BOLD signal accounted for by the model; for details see Glover et al. [2000].

After applying RETROICOR, the BOLD signal was corrected for effects of noncyclic CR processes in two steps. First, the time courses of the noncyclic variables were shifted with multiple lags to account for the variable delay between fluctuations in the BOLD signal and fluctuations in the noncyclic processes. The optimal lags for HR, HRV, and RVT were determined by calculating for every voxel separately, the correlation between the CR time course and the BOLD signal at a range of lags. The optimal lag was then selected as the lag having the strongest absolute correlation. A lag of x means that the values of the CR variable at sample n are compared with the BOLD signal at sample n + x. Lagged signals were shifted in steps of single scans, i.e. by 609 ms. For HRV and RVT the optimal lags were determined in the 0 to 20 s and −10 to 15 s ranges respectively. The negative lags for RVT were included to allow for possible effects of changes in CO_2 on the fMRI signal occurring prior to changes in respiration volume [Birn et al., 2006; Wise et al., 2004]. For HR, lags ran from 0 to 20 s and 0 to 60 s, to account for the peaks of HR - BOLD correlation at two latencies reported by Shmueli et al. [2007]. The lag with the highest correlation in the 0–20 s range was first determined. The optimally lagged signal was regressed out of the BOLD signal to create a temporary residual BOLD time course. Then the lag in the 0–60 s range was determined that gave the highest correlation between HR and the residual BOLD signal.

Second, after the four optimal lags were determined, the BOLD signal was corrected for the effects of the noncyclic processes as follows. The time courses of HR, HRV, and RVT were each shifted with its determined optimal lag (two lags in case of HR) and regressed out of the BOLD signal using multiple regression, for each voxel separately. This CR correction (RETROICOR and additional multiple regression) was performed using custom Matlab software (Aztec, http://www.ni-utrecht.nl/downloads/aztec).

Variance explained by CR correction

The amount of variance explained by RETROICOR and by additional correction for HR, HRV, and respiration volume per time was calculated for the resting-state and task-related BOLD signal. The proportion of explained variance (EV) for each correction was calculated as EV (%) = 100 * (1- ($\sigma_{post}/\sigma_{pre}$)), where σ_{post} was the variance after correction and σ_{pre} variance before correction. This calculation did not take into account the number of regressors included in the model. More specifically, to calculate the variance explained by RETROICOR, the variance after correction with RETROICOR was taken as σ_{post} and the variance in the BOLD signal after applying the high-pass filter was taken as σ_{pre}. To calculate the variance explained by the additional correction, the residual variance after applying this correction was taken as σ_{post} and variance after correction with RETROICOR was taken as σ_{pre}.

Average optimal latency of CR regressors

For descriptive purposes, the average latency which tended to give the strongest correlation between the CR time course and the BOLD signal was calculated for areas of the DMN and task-positive network for each noncyclic variable separately. This was done by taking the average of the optimal lags that were used in the multiple regression analysis of voxels within the DMN and task-positive network. More specifically, these average latencies were calculated by taking first, for each subject, the average of the used optimal lags over voxels within each ROI for both resting-state data and task data. Next, these latencies per ROI were averaged over subjects and over all ROIs within the DMN and within the task-positive network, respectively, to calculate the average latency for each network. Subsequently, these latencies within the DMN and task-positive network for resting-state and the task data were averaged to calculate the average latency of both experiments within the DMN and task-positive network respectively.

Functional Magnetic Resonance Imaging

Measurements

All imaging was performed on a Philips 3.0T Achieva whole-body MRI scanner (Philips Medical Systems, Best, The Netherlands). Functional images were obtained using a 3D PRESTO-SENSE pulse sequence [Neggers et al., 2008] with the following parameters: voxel size 4 mm isotropic, TR = 21.75 ms; TE = 32.4 ms [shifted echo, Liu et al., 1993]; flip angle = 10°; matrix 56 × 64 × 40; field of view 224 × 256 × 160; scan duration 609 ms per 40-slice volume; SENSE-factor R = 2 (anterior-posterior) and R = 1.8 (left-right). This sequence makes use of echo shifting and a multishot 3D acquisition scheme to acquire 40 slices in 609 ms with a TR of 21.75 ms. In echo shifting, the next RF pulse is already applied before the signal acquisition.

Before the functional scans, a reference scan of the same volume of brain tissue was acquired with a high flip-angle (25°) for image coregistration. After the functional images, an 3D fast field echo T1-weighted structural image of the whole brain was made (scan parameters: voxel size 1 mm isotropic, TR = 25 ms; TE = 2.4 ms; flip angle = 30°; field of view 256 × 150 × 204, 150 slices). A total of 750 functional images were acquired during the target detection task (7.5 min) and 592 functional images during the resting-state period (6 min) within two separate dynamic runs.

Image preprocessing

Image preprocessing and analyses were carried out with in-house developed tools and SPM2 (http://www.fil.ion.ucl.ac.uk/spm/). After realignment, the functional scans

were coregistered to the reference scan. The structural scan was also coregistered to the reference scan, thereby providing spatial alignment between the structural and functional volumes. Next, all scans were spatially coregistered to a MNI T1-standard brain and a 3D Gaussian filter (8-mm full width at half maximum) was applied to all functional images.

Analyses

The preprocessed functional images of the target detection task were submitted to a general linear model (GLM) regression analysis. The design matrix contained factors modeling the onsets of the easy (five blocks) and difficult (five blocks) condition as well as the instructions that were presented during the task. These factors were convolved with a canonical hemodynamic response function [Friston et al., 1995]. To correct for drifts in the signal, a high-pass filter (discrete cosine transform basis functions) was applied to the data with a cut-off frequency of 0.007 Hz. Group activation maps were generated for each contrast using a mixed effects analysis [Worsley et al., 2002]. The analyses were repeated for the residual fMRI data after correcting for CR effects. Group activation maps were used to define the regions of interest.

A region of interest (ROI) approach was adopted to test for the effect of task (easy vs. difficult task condition) on BOLD signal changes in DMN regions and a task-positive network. DMN ROIs were defined as regions consisting of voxels showing significant task-related deactivation (i.e. easy and difficult condition relative to rest, $P < 0.05$ Bonferroni corrected) within predefined Brodmann areas (BA), using the automated anatomical labeling atlas [Tzourio-Mazoyer et al., 2002], being the medial prefrontal cortex (MPFC), BA 10), posterior cingulate (PCC, BA 23) and lateral posterior cortices (LP, BA 39). Task-positive ROIs were defined as regions consisting of voxels showing significant task-related activation ($P < 0.05$ corrected) within predefined anatomical regions, being right inferior frontal gyrus (rIFG, BA 45), precentral gyri/supplementary motor area (PCG/SMA, BA 6), right and left fusiform gyri (rFFG and lFFG respectively, BA 19) (Fig. 4A). These areas were found to be active during visual oddball tasks [Kiehl et al., 2001; Yoshiura et al., 1999] and anticorrelated with the PCC [Fox et al., 2005]. The ROIs were used for both the activation and connectivity analyses.

For the activation analyses, the mean regression coefficient (b-value) over all voxels per ROI was calculated for each subject for the contrast easy vs rest and difficult vs rest. These data were entered in SPSS (SPSS Inc.) to perform repeated-measures GLM analyses to test for the effect of task condition (easy, difficult) on activation levels within ROIs of the DMN and the task-positive network before and after correcting for CR effects separately. In addition, repeated-measures GLM analyses were conducted to test for the effect of correction on activation levels within ROIs of the DMN and the task-positive network.

Connectivity analyses

Before the connectivity analyses of the resting-state data, the average whole-brain signal was removed from the preprocessed time series data and the six realignment parameters from rigid body transformation were modeled out of the data through linear regression. This correction was conducted to remove possible global fluctuations that can confound the connectivity analyses. In addition, the data were temporally band-pass filtered (0.01–0.1 Hz) to filter out irrelevant frequency bands. Next, for each subject, the mean residual time series was calculated for each ROI separately, before and after correcting for CR effects.

Correlations within the DMN and the task-positive network were obtained by cross-correlating the mean residual time series data from each ROI with other ROIs of the same network. Per subject, correlation coefficients for each possible pair of ROIs were then converted to a normal distribution by Fisher's z transformation. Subsequently, the mean Fisher's z-score for each pair of ROIs was calculated over subjects. These average group Fisher's z-scores per ROI were then averaged for the DMN and task-positive network.

RESULTS

Behavioral Results

As expected, accuracy was significantly lower for the difficult condition (mean ± SD accuracy, 68.1% ± 14%) compared to the easy condition (mean ± SD accuracy, 99.7% ± 0.8%; $t(13) = 8.49$, $P < 0.0005$). In addition, mean reaction times for correct responses in the difficult condition were significantly longer (mean ± SD, 455 ± 46.9 ms) than in the easy condition (mean ± SD, 401 ± 49.6 ms; $t(13) = 3.46$, $P = 0.004$). We take these results to indicate that the difficult condition was more cognitively demanding than the easy condition.

Cardiorespiratory Processes

Measurements

Before analyzing the fMRI data, a repeated-measures GLM with task condition (three levels; rest, easy, and difficult) as within-subject factor was conducted for each of the following CR variables: HR, HRV and respiration volume per time (see Fig. 2). HR was significantly increased as the task became more difficult (main effect task condition, $F(2,26) = 9.17$, $P = 0.001$), whereas respiration volume and HRV showed a trend towards a significant effect of task condition ($F(2,26) = 2.52$, $P = 0.098$, and $F(2,26) = 2.97$, $P = 0.069$, respectively).

Posthoc paired-sample t-tests showed a significant increase in HR in both the difficult condition ($t(13) = 3.22$, $P = 0.007$) and the easy condition ($t(13) = 3.40$, $P = 0.005$) compared to rest, but not between the two task conditions

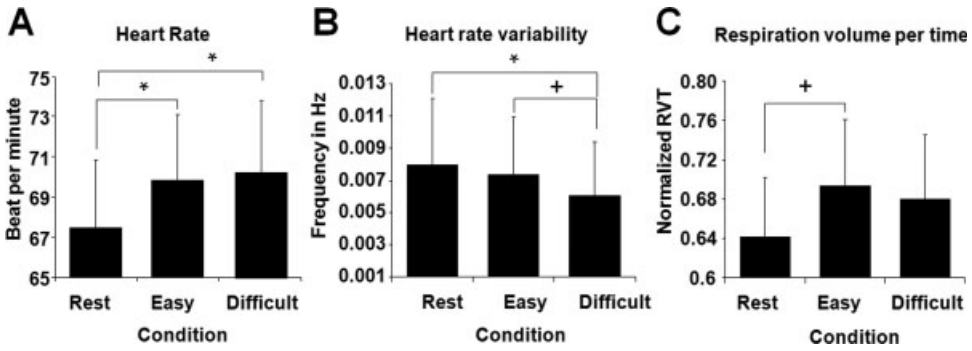

Figure 2.

Cardiorespiratory Measures (**A**) Mean heart rate in beats per minute per condition. (**B**) Mean heart rate variability in frequency (Hz) per condition. (**C**) Mean respiration volume per time (RVT) per condition in scores standardized to maximum and minimum amplitude. * = $P < 0.05$, + = $P < 0.1$. Error bars represent standard error of mean.

($P = 0.393$). A significant decrease in HRV was found in the difficult condition compared to rest ($t(13) = -2.28$, $P = 0.040$) and a trend towards significance was found when comparing the difficult condition to the easy condition ($t(13) = -1.89$, $P = 0.082$). Furthermore, a trend towards a significant increase in respiration volume was found in the easy condition compared to rest ($t(13) = 1.97$, $P = 0.071$).

Explained variance

Next, the impact of CR effects on the BOLD signal within the DMN and task-positive network was investigated by calculating, for each ROI separately, how much of the variance in BOLD signal could be explained by the effects of respiratory and cardiac cycle [RETROICOR; Glover et al., 2000] (see Fig. 3A), and by additional correction for HR, HRV, and respiration volume per time (Fig. 3B). This was done for activation levels (i.e. data acquired during the task, see Table I) and connectivity (i.e. data acquired during resting-state fMRI, see Table II).

During the task, both the amount of variance explained by RETROICOR as well as that explained by additional correction was significantly higher for the task-positive network (20% and 7%) compared to the DMN (15% and 5%) ($t(13) = 6.50$, $P < 0.0005$; $t(13) = 3.22$, $P = 0.007$, respectively). These results indicate that CR effects were less pronounced within the DMN compared to the task-positive network during cognitive task.

The amount of variance explained by RETROICOR during resting-state differed significantly between the DMN (15%) and task-positive network (19%) ($t(13) = -5.38$, $P < 0.0005$), indicating that effects of the respiratory cycle and cardiac pulsation were less present within the DMN compared to the task-positive network during resting-state. The amount of variance explained by additional correction did not differ between the DMN (5%) and task-positive network (6%) ($P = 0.133$).

Latency

For descriptive purposes, we determined for each noncyclic variable separately which latency tended to give the strongest correlation between the CR time course and the BOLD signal. This was done by taking the average of the optimal lags that were used in the CR correction of voxels within the DMN and task-positive network. For respiration volume, two averages were calculated; the average of the used negative optimal lags and the average of the used positive optimal lags.

Changes in the BOLD signal within the ROIs of the DMN were correlated with HRV at an average latency of 9 s (lag 15) and with HR at an average latency of 10 s (lag 16) and 30 s (lag 49). On average, shifting the respiration volume time course with −2 s (lag −3) and 5 s (lag 8) resulted in the strongest correlation with the BOLD signal within the ROIs of the DMN. These average latencies did not differ for the ROIs of the task-positive network ($P > 0.05$). For all noncyclic variables, the correlations at the optimal lags varied over voxels and had a bimodal distribution with peaks around $r = 0.1$ and $r = -0.1$.

BOLD Signal Before Correcting for CR Effects

Activation levels

Two repeated-measures GLM analyses were performed to test for the effect of task condition (easy, difficult) on activation levels within ROIs of the DMN and the task-positive network, respectively, before correcting for CR effects. In ROIs of the DMN (MPFC, PCC, left LP, right LP), deactivation was significantly more pronounced during the difficult task condition compared to the easy condition (main effect of task condition, $F(1,13) = 138.56$, $P < 0.0005$). Furthermore, this task effect differed between ROIs (task condition by ROI interaction, $F(3,11) = 45.32$, $P < 0.0005$). Subsequent paired-sample t-tests showed

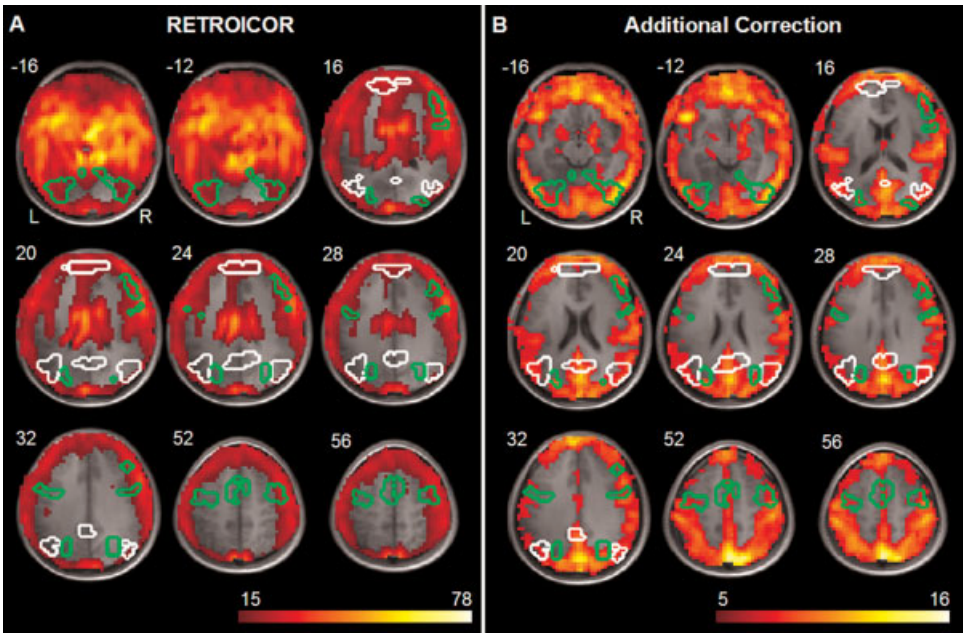

Figure 3.

Explained variance by CR effects (**A**) Average proportion of variance over subjects, in percentages, of resting-state BOLD signal explained by correction for effects of cardiac pulsation and respiratory cycle (RETROICOR), (**B**) Average proportion of variance over subjects, in percentages, of resting-state BOLD signal explained by additional correction for heart rate, heart rate variability, and respiration volume per time (additional correction). Explained variance is overlaid on the mean anatomical image, areas outlined in white represent DMN and outlined in green the task-positive network. The proportion of variance of the BOLD signal during the task explained by cardiac pulsation and respiratory cycle and additional correction for heart rate, heart rate variability, and respiration volume per time yielded similar results. [Color figure can be viewed in the online issue, which is available at www.interscience.wiley.com.]

significantly higher levels of deactivation during the difficult condition compared to the easy condition in the MPFC ($t(13) = 3.22$, $P = 0.007$), the PCC ($t(13) = 13.04$, $P < 0.0005$), and in both the right LP ($t(13) = 7.01$, $P < 0.0005$) and left LP ($t(13) = 10.48$, $P < 0.0005$) (Fig. 4B).

Within ROIs of the task positive network (rIFG, PCG/SMA, rFFG and lFFG), an overall higher level of activation during the difficult task condition compared to the easy condition was found (main effect of task condition, $F(1,13) = 4.98$, $P = 0.044$). This effect differed between the ROIs (task condition by ROI interaction, $F(3,11) = 17.16$, $P < 0.0005$). Subsequent paired-sample t-tests showed a significant increase in activation during the difficult condition compared to the easy condition in the rIFG ($t(13) = 6.47$, $P < 0.0005$) and PCG/SMA ($t(13) = 2.39$, $P = 0.033$). A significant decline in activation was found in the left FFG ($t(13) = -2.24$, $P = 0.043$), whereas activation in the right FFG was not affected by task condition ($P = 0.221$) (Fig. 4C).

Connectivity levels

Average correlations between DMN ROIs differed significantly from zero (Fisher's $z = 0.57$, $t(13) = 11.82$, $P < 0.0005$), indicating that resting-state signal within the DMN was positively correlated (Table III). Average DMN correlation did not differ from that of the task-positive network ($P = 0.511$), indicating that resting-state signals within both networks were equally correlated.

TABLE I. Explained variance during task

	Default-mode network					Task-positive network				
	MPFC	rLP	PCC	lLP	mean	rIFG	PCG	rFFG	lFFG	mean
RETROICOR	28.1 (10.4)	11.4 (3.6)	7.5 (2.7)	11.1 (3.6)	14.5 (4.3)	30.4 (12.4)	17.7 (6.3)	14.6 (5.1)	17.8 (6.4)	20.1 (6.3)
Additional	4.8 (2.6)	4.9 (3.3)	5.4 (3.6)	4.4 (2.7)	4.9 (2.8)	8.0 (4.4)	6.0 (3.1)	6.9 (3.3)	5.7 (2.5)	6.7 (3.1)

Average proportion of variance over subjects within regions of interest, in percentages, explained by correction for the respiratory and cardiac cycle (RETROICOR) and by additional correction for heart rate, heart rate variability and respiration volume per time (additional), standard deviation in brackets.

TABLE II. Explained variance during resting-state

	Default-mode network					Task-positive network				
	MPFC	rLP	PCC	lLP	mean	rIFG	PCG	rFFG	lFFG	mean
RETROICOR	26.5 (9.4)	12.3 (3.9)	7.9 (2.4)	11.2 (3.7)	14.5 (4.1)	28.7 (9.8)	16.8 (6.1)	14.7 (5.8)	17.0 (6.0)	19.3 (5.8)
Additional	5.1 (1.8)	5.6 (2.0)	6.0 (3.3)	4.7 (1.9)	5.4 (2.0)	5.8 (1.9)	5.3 (2.2)	6.9 (3.6)	5.6 (2.8)	5.9 (2.3)

Average proportion of variance over subjects within regions of interest, in percentages, explained by correction for the respiratory and cardiac cycle (RETROICOR) and by additional correction for heart rate, heart rate variability and respiration volume per time (additional), standard deviation in brackets.

BOLD Signal After Correcting for CR Effects

Activation levels

Repeated-measures GLM analyses were performed on the fMRI data after correcting for CR effects for the areas of the DMN and the task-positive network (see Fig. 5A,B). Similar to the results before correction, there was an overall higher level of deactivation during the difficult compared to the easy task condition in DMN ROIs (main effect of task condition, $F(1,13) = 83.95$, $P < 0.0005$), and this effect differed between the ROIs (task condition by ROI interaction, $F(3,11) = 42.68$, $P < 0.0005$). Posthoc paired-sample t-tests showed significantly higher levels of deactivation during the difficult compared to the easy task condition in the PCC ($t(13) = 10.49$, $P < 0.0005$), right LP ($t(13) = 5.44$, $P < 0.0005$), and left LP ($t(13) = 10.60$, $P < 0.0005$). No significant difference in deactivation between the two conditions was found in the MPFC ($P = 0.359$).

ROIs of the task-positive network did not show higher levels of activation during the difficult task condition compared to the easy condition (no main effect of task condition, $P = 0.643$), however the effect of task condition did differ significantly between the ROIs ($F(3,11 = 23.24$, $P < 0.0005$). Subsequent paired-sample t-tests showed a significant increase in activation during the difficult condition compared to the easy condition in the rIFG ($t(13) = 6.58$, $P < 0.0005$). Activation levels in the right FFG and left FFG was significantly lower during the difficult compared

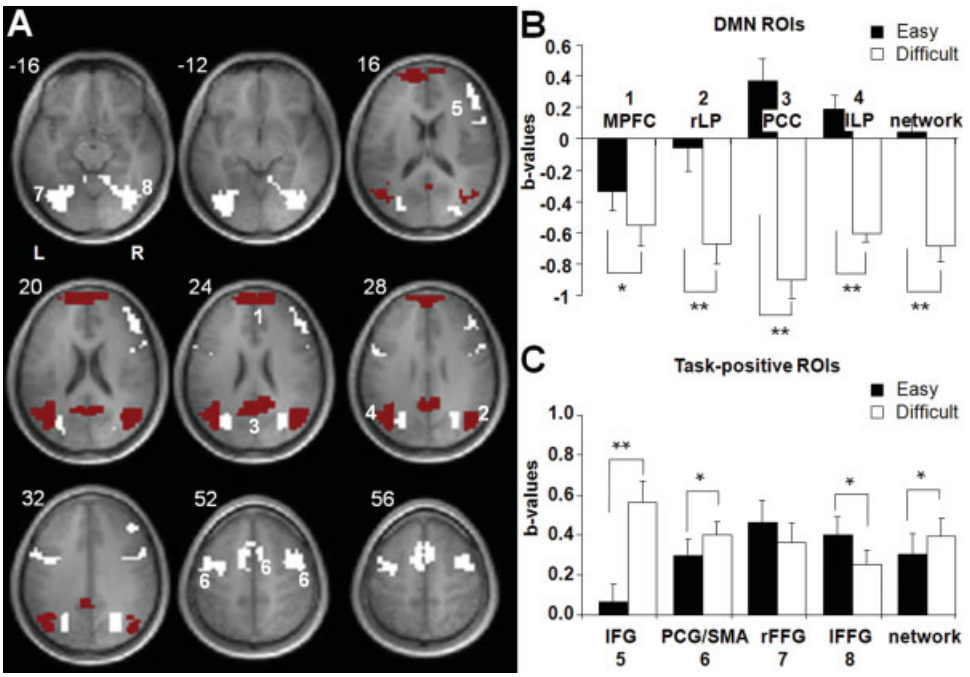

Figure 4.

Activity levels before correcting for CR effects (**A**) ROIs overlaid on the mean anatomical image. Red areas represent DMN and white areas ROIs of the task-positive network. (**B**, **C**) Mean levels of (de)activation in b-values per ROI and overall level of (de)activation in the selected areas during the easy and difficult task condition compared to baseline. Error bars represent standard error of mean. ** = $P < 0.0005$, * = $P < 0.05$. [Color figure can be viewed in the online issue, which is available at www.interscience.wiley.com.]

TABLE III. Resting-state correlations before and after CR correction

ROIs	Fisher's z-score before correction	Fisher's z-score after correction
Default-mode network	0.57**	0.53**
Task-positive network	0.61**	0.53**

Average correlation coefficients during resting-state before and after correcting for CR effects in frequency band from 0.01 to 0.1 Hz. ** = $P < 0.0005$

to the easy condition ($t(13) = -2.04$, $P = 0.061$ and $t(13) = -2.65$, $P = 0.020$, respectively). Activation in the PCG/SMA was not affected by task condition ($P = 0.553$).

Connectivity levels

The average correlation between ROIs of the DMN (Table III) remained significantly different from zero (Fisher's $z = 0.53$, $t(13) = 11.61$, $P < 0.0005$), indicating that the resting-state signal within the DMN was correlated even after correcting for CR effects. Average DMN correlation did not significantly differ from that of the task-positive network ($P = 0.936$), indicating that resting-state signals within the networks were equally correlated.

These analyses were repeated using ROIs based on activation levels after correcting for CR effects and yielded similar results.

Comparison of BOLD Signal Results Before and After Correction

Activation levels

Two repeated-measures GLM analyses were performed to test for the effect of CR correction on activation levels during the two task conditions (easy, difficult) within ROIs of the DMN and the task-positive network, respectively. In ROIs of the DMN, there was a significant lower level of deactivation during the task after correction for CR effects compared to before correction ($F(1,13) = 17.89$, $P = 0.001$). The effect of correction did not differ between ROIs (no correction by ROI interaction, $P = 0.137$). However, the effect of correction did differ between the two task conditions (correction by task condition interaction ($F(1,13) = 34.42$, $P < 0.0005$). Subsequent paired-sample t-tests showed significantly lower levels of deactivation after correcting for CR effects within the DMN during the difficult condition ($t(13) = -4.77$, $P < 0.0005$), but significantly higher levels of activation during the easy condition after correcting for CR effects ($t(13) = 3.02$, $P = 0.009$).

ROIs of the task-positive network displayed overall lower levels of activation during the task after compared to before correcting for CR effects (main effect of correction $F(1,13) = 13.31$, $P = 0.003$). This effect of correction did not differ between ROIs ($P = 0.113$). However, the effect of correction did differ between the two task conditions (correction by task condition interaction $F(1,13) = 7.35$, $P = 0.018$). Subsequent paired-sample t-tests showed significantly lower levels of activation after correcting for CR effects within the task-positive network during the difficult condition ($t(13) = -3.15$, $P = 0.008$) and during the easy condition ($t(13) = -3.603$, $P = 0.003$).

Connectivity levels

A repeated-measures GLM analysis was performed to test for the effect of CR correction on connectivity levels within the networks (DMN and task-positive network). Compared to before correction, there was an overall lower level of correlation after correction ($F(1,13) = 4.83$, $P = 0.046$). This effect of correction did not differ between the two networks (correction by network interaction, $P = 0.278$).

To investigate the effect of the removal of the average whole brain signal on connectivity levels before and after

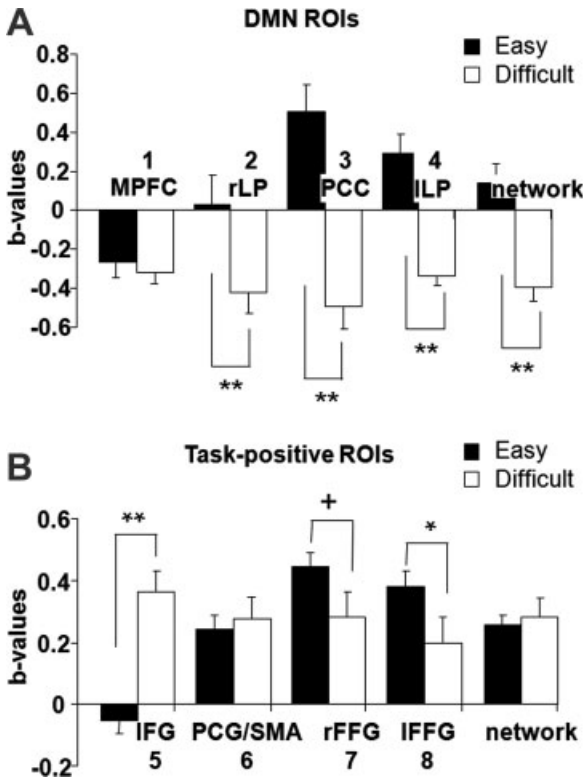

Figure 5.

Activity levels after correcting for CR effects (**A**, **B**) Mean levels of (de)activation in b-values per ROI and overall level of (de)activation in the selected areas during the easy and difficult task condition compared to baseline. Error bars represent standard error of mean. ** = $P < 0.0005$, * = $P < 0.05$, + = $P < 0.1$.

CR correction, all connectivity analyses were rerun without removing the average whole brain signal. These results showed a similar connectivity pattern within the DMN and task-positive network as well as a similar effect of correcting for CR effects.

DISCUSSION

The goal of this study was to investigate whether resting-state and task induced BOLD signal changes within the DMN can be explained by CR effects. To this aim, brain activity, heartbeat, and respiration were measured during resting-state and while subjects performed a cognitive task with two levels (difficult condition, easy condition). We found that correcting for CR effects resulted in both reduced BOLD signal changes during the task (Fig. 5A,B) and reduced resting-state connectivity in the DMN and the task-positive network (Table III) (i.e. areas that showed more activation during the task compared to rest). However, even after applying a strict method to correct for CR effects, BOLD signal changes within the DMN during the task as well as resting-state connectivity between the areas of the DMN remained significant. In addition, DMN deactivation was still modulated by the amount of effort or attention required to perform the task (Fig. 5A). Taken together, these results suggest that the BOLD signal changes within the DMN cannot be explained by CR effects alone and may indeed reflect some form of cognitive neuronal processing.

Birn et al. [2006] and Shmueli et al. [2007] reported CR effects in areas of the DMN. Our results are consistent in that we also found BOLD signal changes within regions of the DMN, namely MPFC, PCC, left and right lateral posterior cortex, to be reduced after correcting for CR effects. However, this reduction also occurred within task-positive regions. In addition, the proportion of variance explained by factors modeling CR effects was higher within the task-positive network compared to DMN. Therefore, no evidence is found in the current study to indicate that CR effects on the BOLD signal are more pronounced within the DMN.

We found a decline in resting-state connectivity between regions of the DMN after correcting for CR effects. However, resting-state connectivity after correction remained significant. This is in concurrence with results of previous studies showing that CR processes affect resting-state signal in general [Dagli et al., 1999; Shmueli et al., 2007; Wise et al., 2004]. Birn et al. [2006] showed that although effects of variations in respiratory volume ($\approx$0.03 Hz) on the BOLD signal were present within the frequency-band of interest ($\approx$0.01–0.1 Hz), connectivity within the DMN was only slightly reduced and remained significant after correcting for these effects.

Earlier studies investigating task-related activation within the DMN have shown that the amount of deactivation within the network is modulated by the effort required to perform the task [Binder et al., 1999; Mason et al., 2007; McKiernan et al., 2003; Singh and Fawcett, 2008]. However, these studies did not correct for possible CR effects, making it difficult to attribute this task demand-related increase in deactivation to cognitive processing alone. In the current study, after correcting for CR effects the task demand-related increase in DMN deactivation remained significant, indicating that BOLD signal changes within the DMN are affected by cognitive processing and reflect neuronal activity. Support for this notion comes from the finding that areas of the DMN are not only functionally but also structurally connected [Greicius et al., 2009]. Furthermore, BOLD signal changes within the DMN were correlated with EEG power within the alpha and beta band [Mantini et al., 2007]. Both these findings suggest that BOLD signal changes within the DMN reflect neuronal activity and make a pure CR explanation for DMN activity unlikely.

Correcting for confounding CR effects will help to more clearly interpret fMRI data of the DMN and to further investigate the processes underlying BOLD signal changes within the DMN. This may be of importance to psychiatric research in particular as this network seems to be disrupted in multiple disorders including schizophrenia [Bluhm et al., 2007; Garrity et al., 2007], ADHD [Castellanos et al., 2008; Uddin et al., 2008] and Alzheimer's disease [Greicius et al. 2004]. In addition, removing CR effects may reduce variance between and within subjects [Raemaekers et al., 2007; Zandbelt et al., 2008].

However, a problem arises if changes in CR processes are correlated with the task the subjects are performing. In that case, correcting for CR effects will also remove some task-related variance. In the current study, we found HR and respiration volume to show task-related differences when comparing the two task conditions to resting periods. Extensive correction for CR effects introduces a trade-off between the interpretability of effects and a potential loss of true but confounded task-related variance. For our purposes, interpretability was essential, and sufficient task-related variance remained within the DMN even after stringent correction.

Recently, correction methods based on component selection through independent component analysis (ICA) or principal component analysis were developed. An advantage of these methods is that they are data-driven and therefore do not require a model of activation or additional measurement of respiration and heart beat [Perlbarg et al., 2007; Behzadi et al., 2007; Tohka et al., 2008; Birn et al., 2008b]. However, most of these techniques only remove effects caused by cardiac pulsation and the respiration cycle, and do not, or only partly, remove variance explained by fluctuations in respiration volume and HR. Furthermore, it is often difficult to identify which components reflect neuronal activity and which components reflect noise. A recent study of Birn et al. [2008b] investigated whether ICA was able to separate the DMN from respiration induced fluctuations by correlating measured

respiration signal with the component identified as the DMN. The study showed that the component identified as the DMN was sometimes similar to the component related to variations in respiration volume and that the DMN-component often still correlated with changes in respiration volume, indicating that ICA cannot completely separate the DMN from respiration induced fluctuations.

The CR correction method used in the current study included regressors to model the major CR processes reported to affect the BOLD signal. The locations in the brain where these CR processes explained most variance, the latency at which these processes affected the BOLD signal as well as the correlations between these processes and the BOLD signal are comparable to findings of previous studies [Birn et al., 2006; Glover et al., 2000; Shmueli et al., 2007]. We argue that our CR correction removed a sufficient proportion of the variance of the BOLD signal to provide an indication that BOLD signal changes within the DMN cannot be explained solely by these CR processes. We base this on the finding that the task-demand related increase in deactivation within the DMN remained significant after correcting the data for CR effects. In contrast, the task-demand related increase in activation within the task-positive network was no longer significant after CR correction. As discussed earlier, this does not necessarily imply that the task-demand related increase in activation before CR correction was caused by CR processes.

A limitation of this study is that only additive linear modelling of the regressors was used in the CR correction. Future studies may benefit from more elaborate modelling of CR processes to account for nonlinear effects of CR processes. Also, it would be useful to further investigate how much additional variance can be explained by including more regressors. In addition, a recent study of Birn et al. [2008a] has reported that in some study paradigms convolving the respiration volume per time regressor with a respiration response function resulted in better fitting of the BOLD signal than assuming a delta function, as was done in the current study.

This study confirmed that part of the BOLD signal within the DMN originates from confounding effects of cardiorespiratory processes. Therefore, appropriate modeling of and correction for cardiorespiratory processes is needed to assess whether neuronal processes drive the BOLD signal within the DMN. After applying such corrections, we still found highly correlated resting-state signal within the DMN, indicating the connectivity within the network is not solely a cardiorespiratory confound. Furthermore, focusing on a demanding task reduces activation within the DMN even after correcting for CR effects, building up evidence for the idea that increased activation within the DMN during rest reflects some form of cognitive processing. In conclusion, our data support the notion that the BOLD signal within the DMN cannot be explained merely by confounding effects of cardiorespiratory processes and is therefore possibly related to some form of cognitive neuronal processing.

REFERENCES

Behzadi Y, Restom K, Liau J, Liu TT (2007): A component based noise correction method (CompCor) for BOLD and perfusion based fMRI. Neuroimage 37:90–101.

Bhattacharyya PK, Lowe MJ (2004): Cardiac-induced physiologic noise in tissue is a direct observation of cardiac-induced fluctuations. Magn Reson Imaging 22:9–13.

Binder JR, Frost JA, Hammeke TA, Bellgowan PSF, Rao SM, Cox RW (1999): Conceptual processing during the conscious resting state: A functional MRI study. J Cogn Neurosci 11:80–93.

Birn RM, Diamond JB, Smith MA, Bandettini PA (2006): Separating respiratory-variation-related fluctuations form neuronal-activity-related fluctuations in fMRI. Neuroimage 31:1536–1548.

Birn RM, Smith MA, Jones TB, Bandettini PA (2008a) The respiration response function: The temporal dynamics of fMRI signal fluctuation related to changes in respiration. Neuroimage 40: 644–654.

Birn RM, Murphy K, Bandettini PA (2008b). The effect of respiration variations on independent component analysis results of resting state functional connectivity. Hum Brain Mapp 29:740–750.

Bluhm RL, Miller J, Lanius RA, Osuch EA, Boksman K, Neufeld RWJ, Théberg J, Schaefer B, Williamson P (2007). Spontaneous low-frequency fluctuations in the BOLD signal in schizophrenic patients: Anomalies in the default network. Schizophr Bull 33: 1004–1012.

Castellanos FX, Margulies DS, Kelly C, Uddin LQ, Ghaffari M, Kirsch A, Shaw D, Shehzad Z, Di Martino A, Biswal B, Sonuga-Barke EJS, Rotrosen J, Adler LA, Milham MP (2008): Cingulate-precuneus interactions: A new locus of dysfunction in adult attention-deficit/hyperactivity disorder. Biol Psychiatry 63:332–337.

Critchley HD, Mathias CJ, Josephs O, O'Doherty J, Zanini S, Dewar B-K, Cipolotti L, Shallice T, Dolan RJ (2003): Human cingulate cortex and autonomic control: Converging neuroimaging and clinical evidence. Brain 126:2139–2152.

Dagli MS, Ingeholm JE, Haxby JV (1999): Localization of cardiac-induced signal change in fMRI. Neuroimage 9:407–415.

Damoiseaux JS, Rombouts SARB, Barkhof F, Scheltens P, Stam CJ, Smith SM, Beckmann CF (2006): Consistent resting-state networks across healthy subjects. Proc Natl Acad Sci USA 103: 13848–13853.

Fox ME, Snyder AZ, Vincent JL, Corbetta M, Van Essen DC, Raichle ME (2005): The human brain is intrinsically organized into dynamic, anticorrelated functional networks. Proc Natl Acad Sci USA 102:9673–9678.

Friston KJ, Frith CD, Turner R, Frackowiak RSJ (1995): Characterizing evoked hemodynamics with fMRI. Neuroimage 2:157–165.

Garrity AG, Pearlson FD, McKiernan K, Lloyd D, Kiehl KA, Calhoun VD (2007): Aberrant "Default Mode" functional connectivity in schizophrenia. Am J Psychiatry 164:450–457.

Glover HG, Li T-Q, Ress D (2000): Image-based method for retrospective correction of physiological motion effects in fMRI: RETROICOR. Magn Reson Med 44:162–167.

Greicius MD, Krasnow B, Reiss AL, Menon V (2003): Functional connectivity in the resting brain: A network analysis of the default mode hypothesis. Proc Natl Acad Sci USA 100:253–258.

Greicius MD, Srivastava G, Reiss AL, Menon V (2004): Default-mode network activity distinguishes Alzheimer's disease from healthy aging: Evidence from functional MRI. Proc Natl Acad Sci USA 101:4637–4642.

Greicius MD, Supekar K, Menon V, Dougherty RF (2009): Resting-state functional connectivity reflects structural connectivity in the default mode network. Cerebral Cortex 19:72–78.

Gusnard DA, Akbudak E, Shulman GL, Raichle ME (2001): Medial prefrontal cortex and self-referential mental activity: Relation to a default mode of brain function. Proc Natl Acad Sci USA 98:4259–4264.

Gusnard DA, Raichle ME (2001): Searching for a baseline: Functional imaging and the resting human brain. Nat Neurosci 2:685–694.

Hu X, Le TH, Parrish T, Erhard P (1995): Retrospective estimation and correction of physiological fluctuation in functional MRI. Magn Reson Med 24:201–212.

Johnson SC, Baxter LC, Wilder LS, Pipe JG, Heiserman JE, Prigatano GP (2002): Neural correlates of self-reflection. Brain 125:1808–1814.

Jorna PGAM (1992): Spectral analysis of heart rate and psychological state: A review of its validity as a workload index. Biol Psychol 34:237–257.

Katura T, Tanaka N, Obata A, Sato H, Maki A (2006): Quantitative evaluation of interrelations between spontaneous low-frequency oscillations in cerebral hemodynamics and systemic cardiovascular dynamics. Neuroimage 31:1592–1600.

Kiehl KA, Laurens KR, Duty TL, Forster BB, Liddle PF (2001): An event-related fMRI study of visual and auditory oddball tasks. J Psychophysiol 15:221–240.

Liu G, Sobering G, Duyn J, Moonen CT (1993): A functional MRI technique combining principles of echo-shifting with a train of observations (PRESTO). Magn Reson Med 30:764–768.

Lowe MJ, Mock BJ, Sorenson JA (1998): Functional connectivity in single and multislice echoplanar imaging using resting-state fluctuations. Neuroimage 7:119–132.

Mantini D, Perrucci MG, Del Gratta C, Romani GL, Corbetta M (2007): Electrophysiological signatures of resting state networks in the human brain. Proc Natl Acad Sci USA 104:13170–13175.

Mason MF, Norton MI, Van Horn JD, Wegner DM, Grafton ST, Macrae CN (2007): Wandering minds: The default network and stimulus-independent thought. Science 315:393–395.

Mazoyer B, Zago L, Mellet E, Bricogne S, Etard O, Houde O, Crivello F, Joliot M, Petit L, Tzourio-Mazoyer N (2001): Cortical networks for working memory and executive functions sustain the conscious resting state in man. Brain Res Bull 54:287–298.

McKiernan KA, Kaufman JN, Kucera-Tompson J, Binder JR (2003): A parametric manipulation of factors affecting task-induced deactivation in functional neuroimaging. J Cogn Neurosci 15: 394–408.

McKiernan KA, D'Angelo BR, Kaufman JN, Binder JR (2006): Interrupting the "stream of consciousness": An fMRI investigation. Neuroimage 29:185–1191.

Neggers SFW, Hermans EJ, Ramsey NF (2008): Enhanced sensitivity by fast 3D BOLD fMRI: Comparison of SENSE-PRESTO and 2D EPI at 3T. NMR Biomed 21:663–676.

Oldfield RC (1971): The assessment and analysis of handedness: The Edinburgh inventory. Neuropsychologia 9:97–113.

Perlbarg V, Bellec P, Anton J-L, Pélégrini-Issac M, Doyon J, Benali H (2007). CORSICA: Correction of structured noise in fMRI by automatic identification of ICA components. Magn Reson Imaging 25:35–46.

Raemaekers M, Vink M, Zandbelt B, van Wezel RJ, Kahn RS, Ramsey NF (2007): Test-retest reliability of fMRI activation during prosaccades and antisaccades. Neuroimage 36:532–542.

Raichle ME, MacLeod AM, Snyder AZ, Powers WJ, Gusnard DA, Shulman GL (2001): A default mode of brain function. Proc Natl Acad Sci USA 98:676–682.

Shmueli K, van Gelderen P, de Zwart JA, Horovitz SG, Fukunaga M, Jansma JM, Duyn JH (2007): Low-frequency fluctuations in the cardiac rate as a source of variance in the resting-state fMRI BOLD signal. Neuroimage 38:306–320.

Shulman GL, Fiez JA, Corbetta M, Buckner RL, Miezin FM, Raichle ME, Petersen SE (1997): Common blood flow changes across visual tasks: II. Decreases in cerebral cortex. J Cogn Neurosci 9:648–663.

Singh KD, Fawcett IP (2008): Transient and linearly graded deactivation of the human default-mode network by a visual detection task. Neuroimage 41:100–112.

Tohka J, Foerde K, Aron AR, Tom SM, Toga AW, Poldrack RA (2008): Automatic independent component labeling for artifact removal in fMRI. Neuroimage 39:1227–1245.

Tzourio-Mazoyer N, Landeau B, Papathanassiou D, Crivello F, Etard O, Delcroix N, Mazoyer B, Joliot M (2002): Automated anatomical labeling of activation in SPM using a macroscopic anatomical parcellation of the MNI MRI single-subject brain. Neuroimage 15:273–289.

Uddin LQ, Kelly AMC, Biswal BB, Margulies DS, Shehzad Z, Shaw D, Ghaffari M, Rotrosen J, Adler LA, Castellanos FX, Milham MP (2008): Network homogeneity reveals decreased integrity of default-mode network in ADHD. J Neurosci Methods 169:249–254.

Wise RG, Ide K, Poulin MJ, Tracey I (2004): Resting fluctuations in arterial carbon dioxide induce significant low frequency variations in BOLD signal. Neuroimage 21:1652–1664.

Worsley KJ, Liao CH, Aston J, Petre V, Duncan GH, Morales F, Evans AC (2002): A general statistical analysis for fMRI data. Neuroimage 15:1–15.

Yoshiura T, Zhong J, Shibata DK, Kwok WE, Shrier DA, Numaguchi Y (1999): Functional MRI study of auditory and visual oddball tasks. Neuroreport 10:1683–1688.

Zandbelt BB, Gladwin TE, Raemaekers M, van Buuren M, Neggers SF, Kahn RS, Ramsey NF, Vink M (2008): Within-subject variation in BOLD-fMRI signal changes across repeated measurements: Quantification and implication for sample size. Neuroimage 42:196–206.